

SpArX: Sparse Argumentative Explanations for Neural Networks

Hamed Ayoobi¹, Nico Potyka¹, Francesca Toni¹

¹Department of Computing, Imperial College London, United Kingdom
 {h.ayoobi, n.potyka, f.toni}@imperial.ac.uk

Abstract

Neural networks (NNs) have various applications in AI, but explaining their decision process remains challenging. Existing approaches often focus on explaining how changing individual inputs affects NNs' outputs. However, an explanation that is consistent with the input-output behaviour of an NN is not necessarily faithful to the actual mechanics thereof. In this paper, we exploit relationships between *multi-layer perceptrons* (MLPs) and *quantitative argumentation frameworks* (QAFs) to create argumentative explanations for the mechanics of MLPs. Our *SpArX* method first sparsifies the MLP while maintaining as much of the original mechanics as possible. It then translates the sparse MLP into an equivalent QAF to shed light on the underlying decision process of the MLP, producing *global and/or local explanations*. We demonstrate experimentally that *SpArX* can give more faithful explanations than existing approaches, while simultaneously providing deeper insights into the actual reasoning process of MLPs.

1 Introduction

The increasing use of black-box models like neural networks (NNs) in autonomous intelligent systems raises concerns about their fairness, reliability and safety. In order to address these concerns, the literature puts forward various explainable AI approaches to make the mechanics of NNs more transparent. This literature includes model-agnostic approaches as in [Ribeiro *et al.*, 2016; Lundberg and Lee, 2017] and approaches tailored to the structure of NNs as in [Bach *et al.*, 2015; Zintgraf *et al.*, 2017]. However, these approaches fail to capture the actual mechanics of the NNs they aim to explain and thus it is hard to evaluate how faithful these approaches are [Heo *et al.*, 2019; Sanchez-Lengeling *et al.*, 2020; Rao *et al.*, 2022].

[Wu *et al.*, 2021] recently proposed regularizing the training procedure of NN such that they can be well approximated by decision trees. While this is an interesting direction, evaluating the faithfulness of the decision trees to the NN remains a challenge. Other recent work unearthed formal relationships between NNs in the form of multi-layer percep-

trons (MLPs) and symbolic reasoning approaches like *quantitative argumentation frameworks* (QAFs) [Potyka, 2021; Ayoobi *et al.*, 2021b; Ayoobi *et al.*, 2021a] and weighted conditional knowledge bases [Giordano and Dupré, 2021]. The formal relationships indicate that these approaches may pave the way towards potentially more faithful explanations than approximate abstractions, such as decision trees.

In this paper, we provide explanations for MLPs leveraging on their formal relationships with QAFs in [Potyka, 2021]. Intuitively, QAFs represent arguments and relations of attack or support between them as a graph, where nodes hold arguments and edges represent the relations. Various QAF formalisms have been studied over the years, e.g. by [Cayrol and Lagasquie-Schiex, 2005; Amgoud *et al.*, 2008; Baroni *et al.*, 2015; Rago *et al.*, 2016; Amgoud *et al.*, 2017; Potyka, 2018; Mossakowski and Neuhaus, 2018; Potyka, 2019]. As it turns out, every MLP corresponds to a QAF of a particular form (where arguments are equipped with a base score and edges with weights) under a particular semantics (ascribing a “dialectical” strength to arguments), and, conversely, many acyclic QAFs corresponds to MLPs [Potyka, 2021]. While this relationship suggests that QAFs are well suited to create faithful explanations for MLPs, it is evident that just reinterpreting an MLP as a QAF would not give us a comprehensible explanation in general because the QAF has the same density as the original MLP.

In order to create faithful and comprehensible argumentative explanations, we propose a novel method based on a two-step process. We first *sparsify* the MLP, while maintaining as much of its mechanics as possible, in the spirit of clustering. Then, we translate the sparse MLP into a QAF, extending the method of [Potyka, 2021]. We call our method *SpArX* (standing for *Sparse Argumentative eXplanations* for MLPs). In principle, in order to sparsify in the first step, we could just apply an existing compression method for NNs (e.g. [Yu *et al.*, 2022]). However, existing methods are not designed for maintaining the mechanics of NNs. We thus make the following contributions:

- We propose a novel *clustering method* for summarizing neurons based on their output-similarity. We compute parameters for the clustered neurons by aggregating the original parameters so that the output of the clustered neuron is similar to the neurons that it summarizes.

- We propose two families of *aggregation functions* for aggregating the parameters of neurons in a cluster: the first gives *global explanations* (explaining the global behaviour of the MLP) and the second gives *local explanations* (explaining the behaviour of the MLP at a target point, when the MLP is applied to a specific input).
- We conduct several experiments demonstrating the viability of our SpArX method for MLPs and its competitiveness with respect to other methods in terms of (i) conventional notions of *input-output faithfulness* of explanations and (ii) novel notions of *structural faithfulness*, while (iii) shedding some light on the tradeoff between faithfulness and comprehensibility understood in terms of a notion of *cognitive complexity*, when generating explanations with SpArX.

Overall, we show that formal relationships between black-box machine learning models (such as NNs) and interpretable symbolic reasoning approaches (such as QAFs) can pave the way toward practical solutions for faithful and comprehensible explanations showing how the models reason.

2 Related Work

While MLPs are most commonly used in their fully connected form, there has been increasing interest in learning sparse NNs in recent years. However, the focus is usually not on finding an easily interpretable network structure, but rather on decreasing the risk for overfitting, memory and runtime complexity and the associated power consumption. Existing approaches include regularization to encourage neurons with weight 0 to be deleted [Louizos *et al.*, 2018], pruning of edges [Yu *et al.*, 2022], compression [Louizos *et al.*, 2017] and low rank approximation [Tai *et al.*, 2016]. Another related approach introduces interval NNs [Prabhakar and Rahimi Afzal, 2019], which summarize neurons in clusters and consider interval outputs for the clustered neurons to give lower and upper bounds on the outputs for verification purposes. Our method is related to interval NNs in that we also summarize neurons in clusters. However, as opposed to [Prabhakar and Rahimi Afzal, 2019], we cluster neurons based on their output. Furthermore, the output associated with a cluster is not an interval, but a numerical value like in a standard MLP. To compute the output, we aggregate the neurons in the cluster using different aggregation functions.

Several approaches exist for obtaining argumentative explanations for a variety of models, e.g. as recently overviewed in [Cyras *et al.*, 2021], including for NNs [Albini *et al.*, 2020; Sukpanichnant *et al.*, 2021], but these are based on approximations of NNs (e.g. using Layerwise Relevance Propagation [Bach *et al.*, 2015]), rather than summarizations as in our method, and their faithfulness is difficult to ascertain.

Several existing methods, like ours, make use of symbolic reasoning approaches for providing explanations, e.g. as recently overviewed in [Marques-Silva and Ignatiev, 2022]. The explanations resulting from these methods (e.g. abduction-based explanations [Ignatiev *et al.*, 2019], prime implicants [Shih *et al.*, 2018], sufficient reasons [Darwiche and Hirth, 2020], and majority reasons [Audemard *et al.*, 2022]) faithfully capture the input-output behaviour of the

explained models rather than their mechanics, as our method does for MLPs. Other methods extract logical rules as explanations for machine learning models, including NNs, e.g. as in [Guidotti *et al.*, 2019] and [Ferreira *et al.*, 2022], but again focus on explanations that are input-output faithful rather than on explaining the underpinning mechanics.

3 Preliminaries

Intuitively, a multi-layer perceptron (MLP) is a layered acyclic graph that processes its input by propagating it through the layers. Formally, we describe MLPs as follows.

Definition 1 (Multi-Layer Perceptron (MLP)). An *MLP* \mathcal{M} is a tuple $(V, E, \mathcal{B}, \mathcal{W}, \varphi)$, where:

- (V, E) is a directed graph;
- $V = \bigcup_{l=0}^{d+1} V_l$ consists of (ordered) layers of neurons; for $0 \leq l \leq d+1$, $V_l = \{v_{l,i} \mid 1 \leq i \leq |V_l|\}$: we call V_0 the *input layer*, V_{d+1} the *output layer* and V_l , for $1 \leq l \leq d$, the l -th *hidden layer*; d is the *depth* of the MLP.
- $E \subseteq \bigcup_{l=0}^d (V_l \times V_{l+1})$ is a set of edges between adjacent layers; if $E = \bigcup_{l=0}^d (V_l \times V_{l+1})$, then the MLP is called *fully connected*;
- $\mathcal{B} = \{b^1, \dots, b^{d+1}\}$ is a set of *bias* vectors, where, for $1 \leq l \leq d+1$, $b^l \in \mathbb{R}^{|V_l|}$;
- $\mathcal{W} = \{W^0, \dots, W^d\}$ is a set of *weight* matrices, where, for $1 \leq l \leq d$, $W^l \in \mathbb{R}^{|V_{l+1}| \times |V_l|}$ such that $W^l_{i,j} = 0$ whenever $(v_{l,j}, v_{l+1,i}) \notin E$;
- $\varphi : \mathbb{R} \rightarrow \mathbb{R}$ is an *activation function*.

In order to process an *input* $x \in \mathbb{R}^{|V_0|}$, the input layer of \mathcal{M} is initialized with x . The input is then propagated forward through the MLP to generate values at each subsequent layer and ultimately an *output* in the output layer. Formally, if the values at layer l are $x_l \in \mathbb{R}^{|V_l|}$, then the values $x_{l+1} \in \mathbb{R}^{|V_{l+1}|}$ at the next layer are defined by $x_{l+1} = \varphi(W^l x_l + b^l)$, where the activation function φ is applied component-wise. We let $\mathcal{O}_x^{\mathcal{M}} : V \rightarrow \mathbb{R}$ denote the *output function* of \mathcal{M} , assigning to every neuron its value when the input x is given. That is, for $v_{0,i} \in V_0$, we let $\mathcal{O}_x^{\mathcal{M}}(v_{0,i}) = x_i$ and, for $l > 0$, we let the *activation value* of neuron $v_{l,i}$ be $\mathcal{O}_x^{\mathcal{M}}(v_{l,i}) = \varphi(W^l \mathcal{O}_x^{\mathcal{M}}(V_{l-1}) + b^l)_i$, where $\mathcal{O}_x^{\mathcal{M}}(V_{l-1})$ denotes the vector that is obtained from V_{l-1} by applying $\mathcal{O}_x^{\mathcal{M}}$ component-wise.

Every MLP can be seen as a quantitative argumentation framework (QAF) [Potyka, 2021]. Intuitively, QAFs are *edge-weighted* directed graphs, where nodes represent *arguments* and, similarly to [Mossakowski and Neuhaus, 2018], edges with negative weight represent *attack* and edges with positive weight represent *support* relations between arguments. Each argument is initialized with a *base score* that assigns an *a priori strength* to the argument. The strength of arguments is then updated iteratively based on the strength values of attackers and supporters until the values converge. In acyclic graphs corresponding to MLPs, this iterative process is equivalent to the forward propagation process in the MLPs [Potyka, 2021]. Conceptually, strength values are from some *domain* \mathcal{D} [Baroni *et al.*, 2018]. As we focus on (real-valued)

MLPs, we will assume $\mathcal{D} \subseteq \mathbb{R}$. The exact domain depends on the activation function, e.g. the logistic function results in $\mathcal{D} = [0, 1]$, the hyperbolic tangent in $\mathcal{D} = [-1, 1]$ and ReLU in $\mathcal{D} = [0, \infty]$. Formally, we describe QAFs as follows.

Definition 2 (Quantitative Argumentation Framework (QAF)). A *QAF* with domain $\mathcal{D} \subseteq \mathbb{R}$ is a tuple $(\mathcal{A}, E, \beta, w)$ that consists of

- a set of *arguments* \mathcal{A} and a set of *edges* $E \subseteq \mathcal{A} \times \mathcal{A}$ between arguments,
- a function $\beta : \mathcal{A} \rightarrow \mathcal{D}$ that assigns *base scores* from \mathcal{D} to all arguments, and
- a function $w : E \rightarrow \mathbb{R}$ that assigns *weights* to all edges.

Edges with negative/positive weights are called *attack/support* edges, denoted by Att/Sup, respectively.

The strength values of arguments are usually computed iteratively using a two-step update procedure [Mossakowski and Neuhaus, 2018]: first, an *aggregation function* α aggregates the strength values of attackers and supporters; then, an *influence function* φ adapts the base score. Examples of aggregation functions include product [Baroni *et al.*, 2015; Rago *et al.*, 2016], addition [Amgoud and Ben-Naim, 2017; Potyka, 2018] and maximum [Mossakowski and Neuhaus, 2018] and the influence function is defined accordingly to guarantee that strength values fall in the domain \mathcal{D} . In this paper, we focus on the aggregation and influence function from [Potyka, 2021], to obtain QAFs simulating MLPs with a logistic activation function [Potyka, 2021]. The strength values of arguments are computed by the following iterative procedure: for every argument $a \in \mathcal{A}$, we let $s_a^{(0)} := \beta(a)$ be the initial strength value; the strength values are then updated by the following two steps repeatedly for all $a \in \mathcal{A}$ (where the auxiliary variable α_a^i carries the aggregate at iteration $i \geq 0$):

Aggregation: $\alpha_a^{(i+1)} := \sum_{(b,a) \in E} w((b, a)) \cdot s_b^{(i)}$.

Influence: $s_a^{(i+1)} := \varphi_l(\ln(\frac{\beta(a)}{1-\beta(a)}) + \alpha_a^{(i+1)})$, where $\varphi_l(z) = \frac{1}{1+\exp(-z)}$ is the logistic function.

The *final strength* of argument a is defined via the limit of $s_a^{(i)}$, for i towards infinity. Notably, the semantics given by this notion of final strength satisfies almost all desiderata for QAF semantics perfectly [Potyka, 2021].

4 From General MLPs to QAFs

Here we generalize the connection between MLPs and QAFs beyond MLPs with logistic activation functions, as follows. Assume that $\varphi : \mathbb{R} \rightarrow \mathcal{D}$ is an activation function that is strictly monotonically increasing. Examples include logistic, hyperbolic tangent and parametric ReLU activation functions. Then φ is invertible and $\varphi^{-1} : \mathcal{D} \rightarrow \mathbb{R}$ is defined. We can then define the update function corresponding to an MLP with such activation function φ by using the same aggregation function as before and using the following influence function:

Influence: $s_a^{(i+1)} := \varphi(\varphi^{-1}(\beta(a)) + \alpha_a^{(i+1)})$.

Note that the previous definition of influence in Section 3, from [Potyka, 2021], is a special case because $\ln(\frac{1}{1-x})$ is

the inverse function of the logistic function $\varphi_l(x)$. Note also that the popular ReLU activation function $\varphi_{ReLU}(x) = \max(0, x)$ is not invertible because all non-positive numbers are mapped to 0. However, for our purpose of translating MLPs to QAFs, we can define

$$\varphi_{ReLU}^{-1}(x) = \begin{cases} x, & \text{if } x > 0; \\ 0, & \text{otherwise.} \end{cases}$$

In order to translate an MLP \mathcal{M} with activation function φ and input x into a QAF $Q_{\mathcal{M},x}$, we interpret every neuron $v_{l,i}$ as an abstract argument $A_{l,i}$. Edges in \mathcal{M} with positive/negative weights are interpreted as supports/attacks, respectively, in $Q_{\mathcal{M},x}$. The base score of an argument $A_{0,i}$ associated with input neuron $v_{0,i}$ is just the corresponding input value x_i . The base score of the remaining arguments $A_{l,i}$ is $\varphi(b_i^l)$, where b_i^l is the bias of the associated neuron $v_{l,i}$.

Proposition 1. Let \mathcal{M} be an MLP with activation function φ that is invertible or ReLU. Then, for every input x , the QAF $Q_{\mathcal{M},x}$ satisfies $\mathcal{O}_x^{\mathcal{M}}(v_{l,i}) = \sigma(A_{l,i})$, where $\sigma(A_{l,i})$ denotes the final strength of $A_{l,i}$ in $Q_{\mathcal{M},x}$.

5 SpArX: Explaining MLPs with QAFs

Just translating an MLP into a QAF would not give a comprehensible explanation in general because the QAF has the same density as the original MLP. Thus, in order to explain an MLP, we first sparsify it, in a customizable way to support different comprehensibility needs, and then translate it into a QAF. The sparsification should maintain as much of the original MLP as possible to give faithful explanations. To achieve this, roughly speaking we exploit redundancies in the MLP by replacing neurons giving similar outputs with a single neuron that summarizes their joint effect.

Summarizing neurons in this way is a clustering problem. Formally, a clustering problem is defined by a set of inputs from an abstract space \mathcal{S} and a distance measure $\delta : \mathcal{S} \times \mathcal{S} \rightarrow \mathbb{R}_{\geq 0}$. The goal is to partition \mathcal{S} into clusters C_1, \dots, C_K (where $\mathcal{S} = \bigcup_{i=1}^K C_i$) such that the distance between points within a cluster is 'small' and the distance between points in different clusters is 'large'. Finding an optimal clustering is NP-complete in many cases [Gonzalez, 1982]. Thus, we cannot expect to find an efficient algorithm that computes an optimal clustering, but we can apply standard algorithms e.g. K-means [MacQueen, 1967] to find a good (but not necessarily optimal) clustering efficiently.

In our setting, \mathcal{S} is the set V_l of neurons in any given layer $0 < l < d + 1$ and the distance between two neurons can be defined as the difference between their outputs for the inputs in a given dataset Δ (e.g. the training dataset):

$$\delta(v_{l,i}, v_{l,j}) = \sqrt{\sum_{x \in \Delta} (\mathcal{O}_x^{\mathcal{M}}(v_{l,i}) - \mathcal{O}_x^{\mathcal{M}}(v_{l,j}))^2}. \quad (1)$$

After clustering, we have a partitioning $\mathcal{P} = \bigcup_{l=1}^d \mathcal{P}_l$ of (the hidden layers of) our MLP \mathcal{M} , where $\mathcal{P}_l = \{C_1^l, \dots, C_{K_l}^l\}$ is the clustering of the l -th layer, that is, $V_l = \bigcup_{i=1}^{K_l} C_i^l$. We use the clustering to create a corresponding *clustered MLP* μ whose neurons correspond to clusters in the original \mathcal{M} . We

call these neurons *cluster-neurons* and denote them by v_C , where C is the associated cluster. The graphical structure of μ is as follows.

Definition 3 (Graphical Structure of Clustered MLP). Given an MLP \mathcal{M} and a clustering $\mathcal{P} = \sqcup_{i=1}^d \mathcal{P}_i$ of \mathcal{M} , the *graphical structure of the corresponding clustered MLP μ* is a directed graph (V^μ, E^μ) such that

- $V^\mu = \sqcup_{l=0}^{d+1} V_l^\mu$ consists of (ordered) layers of cluster-neurons such that:
 1. the input layer V_0^μ consists of a singleton cluster-neuron $v_{\{v_{0,i}\}}$ for every input neuron $v_{0,i} \in V_0$;
 2. the l -th hidden layer of μ (for $0 < l < d+1$) consists of one cluster-neuron v_C for every cluster $C \in \mathcal{P}_l$;
 3. the output layer V_{d+1}^μ consists of a singleton cluster-neuron $v_{\{v_{d+1,i}\}}$ for every output neuron $v_{d+1,i} \in V_{d+1}$;
- $E^\mu = \bigcup_{l=0}^d (V_l^\mu \times V_{l+1}^\mu)$.

Example 1. For illustration, consider the MLP in Figure 1.a, trained to approximate the XOR function from the dataset $\Delta = \{(0, 0), (0, 1), (1, 0), (1, 1)\}$ with target outputs $0, 1, 1, 0$, respectively. The activation values of the hidden neurons for the four input pairs are $(0, 0, 0, 0), (1.7, 0, 1.8, 0), (0, 2.3, 0, 1.5), (0, 0, 0, 0)$, respectively. Applying K -means clustering with δ as in Eq. 1 and $K = 2$ for the hidden layer results in two clusters C_1, C_2 , indicated by rectangles in the figure.

We define global and local explanations for MLPs by translating their corresponding clustered MLPs into QAFs. The clustered MLPs for global and local explanations share the same graphical structure but differ in the parameters of the cluster-neurons, that is, (i) the biases of cluster-neurons and (ii) the weights for edges between cluster-neurons. We define these parameters in terms of *aggregation functions*, specifically a *bias aggregation function* $\text{Agg}^b : \mathcal{P} \rightarrow \mathbb{R}$, mapping clusters to biases, and an *edge aggregation function* $\text{Agg}^e : \mathcal{P} \times \mathcal{P} \rightarrow \mathbb{R} \cup \{\perp\}$, mapping pairs of clusters to weights if the pairs correspond to edges in μ , or \perp otherwise. Given any concrete such aggregation functions (as defined later), the parameters of μ can be defined as follows.

Definition 4 (Parameters of Clustered MLP). Given an MLP $\mathcal{M} = (V, E, \mathcal{B}, \mathcal{W}, \varphi)$, let (V^μ, E^μ) be the graphical structure of the corresponding clustered MLP μ . Then, for bias and edge aggregation functions Agg^b and Agg^e , respectively, μ is $(V^\mu, E^\mu, \mathcal{B}^\mu, \mathcal{W}^\mu, \varphi)$ with parameters $\mathcal{B}^\mu, \mathcal{W}^\mu$ as follows:

- for every cluster-neuron $v_C \in V^\mu$, the bias (in \mathcal{B}^μ) of v_C is $\text{Agg}^b(C)$;
- for every edge $(v_{C_1}, v_{C_2}) \in E^\mu$, the weight (in \mathcal{W}^μ) of the edge is $\text{Agg}^e((C_1, C_2))$.

5.1 Sparse Argumentative Global Explanations

We consider the following aggregation functions. As we explain in the supplementary material (SM), they minimize the deviation (with respect to the least-squares error) of bias and weights of the cluster neuron and the neurons contained in the cluster.

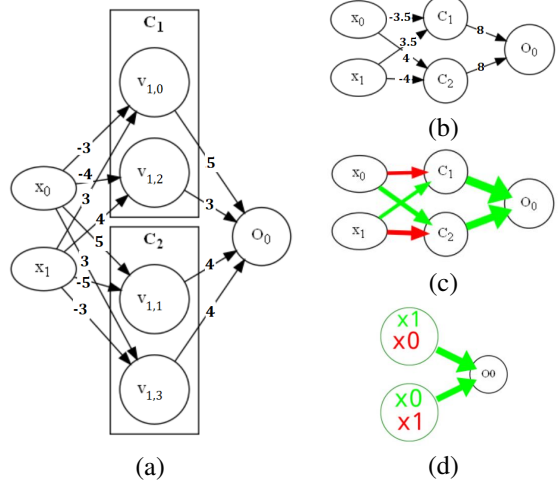


Figure 1: a) MLP for XOR, with cluster-neurons C_1 and C_2 . b) Clustered MLP. c) Global explanation as a QAF. d) Word-cloud representation of the hidden cluster-neurons.

Definition 5 (Global Aggregation Functions). The *average bias* and *edge aggregation functions* are, respectively:

$$\text{Agg}^b(C) = \frac{1}{|C|} \sum_{v_{l,i} \in C} b_i^l;$$

$$\text{Agg}^e((C_1, C_2)) = \sum_{v_{l,i} \in C_1} \frac{1}{|C_2|} \sum_{v_{l+1,j} \in C_2} W_{j,i}^l.$$

The average bias aggregation function simply averages the biases of neurons in the cluster. Intuitively, the weight of an edge between cluster-neurons v_{C_1} and v_{C_2} has to capture the effects of all neurons summarized in C_1 on neurons summarized in C_2 . The neurons in C_1 all affect every neuron in C_2 , therefore their effects have to be summed up. As v_{C_2} acts as a replacement of all neurons in C_2 , it has to aggregate their activation. We achieve this aggregation by averaging again.

The following example illustrates global explanations drawn from clustered MLPs, with the average aggregation functions, via their understanding as QAFs.

Example 2. Figure 1.b shows the clustered MLP for our XOR example from Figure 1.a. The corresponding QAF can be visualised as in Figure 1.c, where attacks are given in red and supports in green, and the thickness of the edges reflects their weight. To better visualize the role of each cluster-neuron, we can use a word-cloud representation as in Figure 1.d (showing, e.g., that x_0 and x_1 play a negative and positive role, respectively, towards C_1 , which supports the output). The word-cloud representation gives insights into the reasoning of the MLP (with the learned rule $(\bar{x}_0 \wedge x_1) \vee (x_0 \wedge \bar{x}_1)$).

5.2 Sparse Argumentative Local Explanations

While global explanations attempt to faithfully explain the behaviour of the MLP on all inputs, our local explanations focus on the behaviour in the neighborhood of the input x from the dataset Δ , similar to LIME [Ribeiro *et al.*, 2016]. To do so, we generate random neighbors of x to obtain a *sample dataset* Δ' , and weigh them with an exponential kernel

from LIME [Ribeiro *et al.*, 2016], assigning lower weight to a sample $x' \in \Delta'$ that is further away from the target x :

$$\pi_{x',x} = \exp(-D(x',x)^2/\sigma^2)$$

where D is the Euclidean distance function and σ is the width of the exponential kernel.

We aggregate biases as before but replace the edge aggregation function with the following.

Definition 6 (Local Edge Aggregation Function). The *local edge aggregation function* with respect to the *input* x is

$$\begin{aligned} \text{Agg}_x^e(C_1, C_2) = \\ \sum_{x' \in \Delta'} \pi_{x',x} \sum_{v_{l,i} \in C_1} \frac{1}{|C_2| \cdot \mathcal{O}_{x'}^\mu(v_{C_1})} \sum_{v_{l+1,j} \in C_2} W_{i,j}^l \mathcal{O}_{x'}^\mathcal{M}(v_{l,i}) \end{aligned}$$

where $\mathcal{O}_{x'}^\mathcal{M}(v_{l,i})$ is the activation value of the neuron $v_{l,i}$ in the original MLP and $\mathcal{O}_{x'}^\mu(v_{C_1})$ is the activation value of the cluster-neuron C_1 in the clustered MLP.

Note that, by this definition, the edge weights are computed layer by layer from input to output.

6 Desirable Properties of Explanations

In order to evaluate SpArX, we consider three measures for assessing faithfulness and comprehensibility of explanations. In this section, we assume as given an MLP \mathcal{M} of depth d and a corresponding clustered MLP μ .

To begin with, we consider a *faithfulness* measure inspired by the notion of fidelity considered for LIME [Ribeiro *et al.*, 2016], based on measuring the *input-output* difference between the original model (in our case, \mathcal{M}) and the substitute model (in our case, the clustered MLP/QAF).

Definition 7 (Input-Output Unfaithfulness). The *local input-output unfaithfulness* of μ to \mathcal{M} with respect to *input* x and *dataset* Δ is

$$\mathcal{L}^\mathcal{M}(\mu) = \sum_{x' \in \Delta} \pi_{x',x} \sum_{v \in V_{d+1}} (\mathcal{O}_{x'}^\mathcal{M}(v) - \mathcal{O}_x^\mu(v))^2.$$

The *global input-output unfaithfulness* of μ to \mathcal{M} with respect to dataset Δ is

$$\mathcal{G}^\mathcal{M}(\mu) = \sum_{x' \in \Delta} \sum_{v \in V_{d+1}} (\mathcal{O}_{x'}^\mathcal{M}(v) - \mathcal{O}_{x'}^\mu(v))^2.$$

The lower the input-output unfaithfulness of the clustered MLP μ , the more faithful μ is to the original MLP.

The input-output unfaithfulness measures deviations in the input-output-behaviour of the substitute model, but, since clustered MLPs maintain much of the structure of the original MLPs, we can define a more fine-grained notion of *structured faithfulness* by comparing the outputs of the individual neurons in the MLP to the output of the cluster-neurons summarizing them in the clustered MLP.

Definition 8 (Structural Unfaithfulness). Let K_l be the number of clusters at hidden layer l in μ ($0 < l \leq d$) and K_{d+1} be the number of output neurons (in μ and \mathcal{M}). Let $K_{l,j}$ be the number of neurons in the j th cluster-neuron $C_{l,j}$ ($0 < l \leq d + 1$,

with $K_{d+1,j} = 1$). Then, the *local structural unfaithfulness* of μ to \mathcal{M} with respect to *input* x and *dataset* Δ is:

$$\mathcal{L}_s^\mathcal{M}(\mu) = \sum_{x' \in \Delta} \pi_{x',x} \sum_{l=1}^{d+1} \sum_{j=1}^{K_l} \sum_{v_{l,i} \in C_{l,j}} (\mathcal{O}_{x'}^\mathcal{M}(v_{l,i}) - \mathcal{O}_{x'}^\mu(v_{l,i}))^2.$$

The *global structural unfaithfulness* $\mathcal{G}_s^\mathcal{M}(\mu)$ is defined analogously by removing the similarity terms $\pi_{x',x}$.

The lower the structured unfaithfulness of the clustered MLP μ , the more structurally faithful μ is to the original MLP. Note that our notion of structural faithfulness is different from the notions of structural descriptive accuracy by [Albini *et al.*, 2022]: they characterise bespoke explanations, defined therein, of probabilistic classifiers equipped with graphical structures and cannot be used in place of our notion, tailored to local and global explanations

Finally, we consider the *cognitive complexity* of an explanation based on its size, inspired by the notion of cognitive tractability in [Cyras *et al.*, 2019]. In our case, we use the number of cluster-neurons/arguments as a measure.

Definition 9 (Cognitive Complexity). Let K_l be the number of clusters at hidden layer l in μ ($0 < l \leq d$). Then, the *cognitive complexity* of μ is defined as

$$\Omega(\mu) = \prod_{0 < l < d+1} K_l$$

Note that there is a tradeoff between faithfulness and cognitive complexity in SpArX. By reducing the number of cluster-neurons, we reduce cognitive complexity. However, this also results in a higher variance in the neurons that are summarized in the clusters, so the faithfulness of the explanation can suffer. We will explore this trade-off experimentally next.

Finally, note that other properties of explanations by symbolic approaches, notably by [Amgoud and Ben-Naim, 2022], are unsuitable for our mechanistic explanations as QAFs. Indeed, these properties characterize the input-output behaviour of classifiers, rather than their mechanics.

7 Experiments

We conducted four sets of experiments to evaluate SpArX with respect to (i) the trade-off between its sparsification and its ability to maintain faithfulness (Section 7.1 for global and Section 7.2 for local explanations), (ii) SpArX’s scalability (Section 7.3), and (iii) the tradeoff between faithfulness and cognitive complexity (Section 7.4). We used four datasets for classification: *iris*¹ with 150 instances, 4 continuous features and 3 classes; *breast cancer*² with 569 instances, 30 continuous features and 2 classes; *COMPAS* [Jeff Larson and Angwin, 2016] with 11,000 instances and 52 categorical features, to classify *two_year_recid*; and *forest covertype*³ [Blackard and Dean, 1999] with 581,012 instances, 54 features (10 continuous, 44 binary), and 7 classes.

We used the first three datasets to evaluate the (input-output and structural) unfaithfulness of the global and local explanations generated by SpArX. We then used the last dataset,

¹<https://archive.ics.uci.edu/ml/datasets/iris>

²<https://archive.ics.uci.edu/ml/datasets/cancer>

³<https://archive.ics.uci.edu/ml/datasets/covertype>

which is considerably larger and requires deeper MLPs with varying architectures, to evaluate the scalability of SpArX. Finally, we used COMPAS to assess cognitive complexity.

For the experiments with the first three datasets we used MLPs with 2 hidden layers and 50 hidden neurons each, whereas for the experiments with the last we used 1-5 hidden layers with 100, 200 or 500 neurons. For all experiments, we used the RELU activation function for the hidden neurons and the softmax activation function for the output neurons. We give classification performances for all MLPs and average run-times for generating local explanations in the SM.

When experimenting with SpArX, one needs to choose the number of clusters/cluster-neurons at each hidden layer: we do so by specifying a *compression ratio* (for example, a compression ratio of 0.5 amounts to obtaining half cluster-neurons than the original neurons).

7.1 Global Faithfulness (Comparison to HAP)

Since SpArX essentially compresses an MLP to construct a QAF, one may ask how it compares to existing compression approaches.⁴ To assess the faithfulness of our global explanations, we compared SpArX’s clustering approach to the state-of-the-art compression method Hessian Aware Pruning (HAP) [Yu *et al.*, 2022], which uses relative Hessian traces to prune insensitive parameters in NNs. We measured both input-output and structural unfaithfulness of SpArX and HAP to the original MLP, using the result of HAP compression in place of μ when applying Definitions 7 and 8 for comparison.

Input-Output Faithfulness. Table 1 shows the input-output unfaithfulness of the global explanations ($\mathcal{G}^{\mathcal{M}}(\mu)$ in Def. 7) obtained from SpArX and HAP using our three chosen datasets and different compression ratios. The unfaithfulness of global explanations in SpArX is lower than HAP especially when the compression ratio is high. Note that this does not mean that SpArX is a better compression method, but that the compression method in SpArX is better for our purposes (that is, compressing the MLP while keeping its mechanics).

Method	Compression		Datasets		
	Ratio		Iris	Cancer	COMPAS
HAP	0.2		0.05	0.48	0.02
SpArX	0.2		0.00	0.02	0.00
HAP	0.4		0.23	0.53	0.11
SpArX	0.4		0.00	0.05	0.00
HAP	0.6		0.23	0.58	0.20
SpArX	0.6		0.00	0.10	0.00
HAP	0.8		0.28	1.00	0.26
SpArX	0.8		0.00	0.21	0.00

Table 1: Global input-output unfaithfulness of sparse MLPs generated by HAP vs our SpArX method. (Best results in **bold**)

⁴Whereas existing NN compression methods typically retrain after compression, we do not, as we want to explain the original NN.

Method	Compression		Datasets		
	Ratio		Iris	Cancer	COMPAS
HAP	0.2		0.23	9.54	0.10
SpArX	0.2		0.00	0.83	0.02
HAP	0.4		0.89	61.57	0.24
SpArX	0.4		0.00	1.04	0.03
HAP	0.6		1.37	61.57	0.46
SpArX	0.6		0.00	1.40	0.04
HAP	0.8		3.00	116.20	1.20
SpArX	0.8		0.02	2.34	0.05

Table 2: Global structural unfaithfulness of sparse MLPs generated by HAP vs our SpArX method.

Method	Datasets		
	Iris	Cancer	COMPAS
LIME	0.3212	0.1623	0.0224
SpArX (0.6)	0.0257	0.0055	0.0071
SpArX (0.8)	0.0707	0.0156	0.0083

Table 3: Local input-output unfaithfulness of LIME vs our SpArX method (with different compression ratios, in brackets).

Structural Faithfulness. Table 2 gives the structural global unfaithfulness ($\mathcal{G}_s^{\mathcal{M}}(\mu)$ in Def. 8) for SpArX and HAP, on the three chosen datasets, using different compression ratios. Our method has a much lower structural unfaithfulness than HAP by preserving activation values close to the original model.

7.2 Local Faithfulness (Comparison to LIME)

In order to evaluate the local input-output unfaithfulness of SpArX ($\mathcal{L}^{\mathcal{M}}(\mu)$ in Def. 7), we compare SpArX and LIME [Ribeiro *et al.*, 2016]⁵, which approximates a target point locally by an interpretable substitute model.⁶ Table 3 shows the input-output unfaithfulness of the local explanations for LIME and SpArX. We used the same sampling approach as LIME [Ribeiro *et al.*, 2016]. We averaged the unfaithfulness measure for all test examples. The results show that the local explanations produced by our approach are more input-output faithful to the original model. Thus, basing local explanations on keeping the MLP mechanics helps also with their input-output faithfulness.

7.3 Scalability

To evaluate the scalability of SpArX, we measured its input-output faithfulness on MLPs of increasing complexity. we have compared it to LIME [Ribeiro *et al.*, 2016] using forest covertype as a sufficiently large dataset to be tested with various MLP architectures with different sizes. We have trained 15 MLPs with varying numbers of hidden

⁵<https://github.com/marcotcr/lime>

⁶We used ridge regression, suitable with tabular data in LIME. We used the substitute model as μ when applying Def. 7 to LIME.

#Layers	Method	#Neurons		
		100	200	500
1	LIME	0.2375	0.2919	0.3123
1	SpArX	0.0000	0.0018	0.0000
2	LIME	0.2509	0.2961	0.3638
2	SpArX	0.0019	0.0015	0.0034
3	LIME	0.3130	0.3285	0.3127
3	SpArX	0.0028	0.0026	0.0000
4	LIME	0.3395	0.3459	0.3243
4	SpArX	0.0001	0.0049	0.0000
5	LIME	0.3665	0.3178	0.3288
5	SpArX	0.0030	0.0064	0.0000

Table 4: Evaluating scalability of SpArX (forest covtype dataset): local input-output unfaithfulness of SpArX (with 80% compression ratio) and LIME using various MLPs with different numbers of hidden layers (#Layers) and neurons (#Neurons).

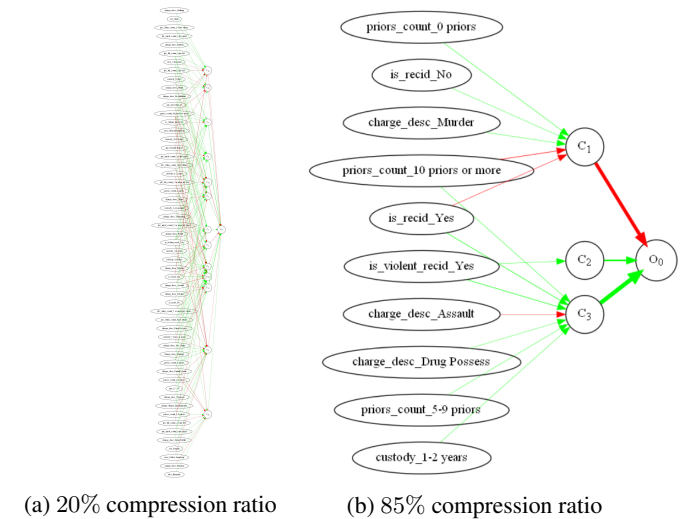
layers (#Layers) and different numbers of hidden neurons (#Neurons) at each hidden layer (see details in the SM).

Table 4 compares the input-output unfaithfulness of the local explanations of SpArX using 80% compression ratio⁷ with LIME, all averaged over the test set. The result confirms that SpArX explanations are scalable to different MLP architectures with different sizes and large datasets.

7.4 Cognitive Complexity

The cognitive complexity of SpArX (Def. 9) is dependent on the number of clusters at each layer. A lower number of clusters leads to a more interpretable explanation at the cost of achieving lower (structural) faithfulness.

Figure 2a shows a *global explanation*⁸ of an MLP for the COMPAS dataset, with one hidden layer and 20 neurons in the hidden layer, with 20% compression ratio and pruning edges with low weights. Note that pruning is only done here for visualization. This explanation is hardly interpretable for a user. The classification results of the clustered MLP is 98.32%, the same as the original MLP. Figure 2b shows the global explanation of the same MLP but with 85% compression rate and pruning the edges with low weights. This global explanation is more comprehensible for humans since there are fewer neurons in the clustered MLP. The classification results of the clustered MLP is 94.60%, the same as the original model. Unlike shallow input-output explanations, we can see the role of each hidden neuron in the proposed method. The output O_0 is *two-year_recid*. There are two sets of hidden cluster-neurons, namely an attacker (C_1) and two supporters (C_2 and C_3). C_1 attacks the output which means the criminal will not recommit a crime in a two-year period. Three features are supporting C_1 and two features are attacking it. The attacking features also support C_3 . This means that they strengthen the support by C_3 and weaken the attack by C_1 . Therefore, *priors_count_10 priors or more* and *is_recid_Yes* both strongly af-



(a) 20% compression ratio

(b) 85% compression ratio

Figure 2: Global explanations by SpArX of an MLP with 20% and 85% compression ratios for the COMPAS dataset.

fect the output. Indeed, looking at the COMPAS dataset, more than 99% of criminals that have these two features recommitted the crime in a two years period. C_2 and C_3 are supporting the output. C_2 is only supported by the *is_violent_recid_Yes* feature. This means that if a criminal has a violent recidivism (s)he will probably recommit a crime after two years. Checking the COMPAS dataset, this interpretation is 100% correct. These kinds of interpretations are beyond the shallow input-output explanations offered by model-agnostic explanation methods such as LIME. C_3 is supported by several features and is attacked by one feature. Looking at this argumentative global explanation one can understand the effect of each feature as well as of each hidden neuron on the output.

8 Conclusion

We introduced SpArX, a novel method for generating sparse argumentative explanations for MLPs. In contrast to shallow input-output explainers like LIME, SpArX focuses on maintaining structural similarity to the original MLP in order to give faithful explanations, while allowing tailoring them to the cognitive needs of users. Our experimental results show that the explanations by SpArX are more (input-output) faithful to the original model than LIME. We have also compared SpArX with a state-of-the-art NN compression technique called HAP, showing that SpArX is more faithful to the original model. Further, our explanations are more *structurally* faithful to the original model by providing deeper insights into the mechanics thereof.

Future research includes extending SpArX to other types of NNs, e.g. CNNs, as well as furthering it to cluster neurons across hidden layers. It would also be interesting to explore whether SpArX could be extended to exploit formal relationships between NNs and other symbolic approaches, e.g. in [Giordano and Dupré, 2021]. Further, it would be interesting to explore formalizations such as in [Liu and Lorini, 2021] for characterizing uncertainty as captured by SpArX.

⁷For experiments with lower compression ratios see the SM.

⁸We give an example of local explanation in the SM.

References

[Albini *et al.*, 2020] Emanuele Albini, Piyawat Lertvitayakumjorn, Antonio Rago, and Francesca Toni. DAX: deep argumentative explanation for neural networks. *CoRR*, abs/2012.05766, 2020.

[Albini *et al.*, 2022] Emanuele Albini, Antonio Rago, Pietro Baroni, and Francesca Toni. Descriptive accuracy in explanations: The case of probabilistic classifiers. In *Scalable Uncertainty Management - 15th International Conference, SUM 2022*, 2022.

[Amgoud and Ben-Naim, 2017] Leila Amgoud and Jonathan Ben-Naim. Evaluation of arguments in weighted bipolar graphs. In *European Conference on Symbolic and Quantitative Approaches to Reasoning with Uncertainty (ECSQARU)*, 2017.

[Amgoud and Ben-Naim, 2022] Leila Amgoud and Jonathan Ben-Naim. Axiomatic foundations of explainability. In *Proceedings of the Thirty-First International Joint Conference on Artificial Intelligence, IJCAI 2022*, 2022.

[Amgoud *et al.*, 2008] Leila Amgoud, Claudette Cayrol, Marie-Christine Lagasque-Schiex, and Pierre Livet. On bipolarity in argumentation frameworks. *International Journal of Intelligent Systems*, 23(10):1062–1093, 2008.

[Amgoud *et al.*, 2017] Leila Amgoud, Jonathan Ben-Naim, Dragan Doder, and Srdjan Vesic. Acceptability semantics for weighted argumentation frameworks. In *Proceedings of the Twenty-Sixth International Joint Conference on Artificial Intelligence, IJCAI 2017*, 2017.

[Audemard *et al.*, 2022] Gilles Audemard, Steve Bellart, Louenas Bounia, Frédéric Koriche, Jean-Marie Lagniez, and Pierre Marquis. Trading complexity for sparsity in random forest explanations. In *Thirty-Sixth AAAI Conference on Artificial Intelligence, AAAI 2022*, 2022.

[Ayoobi *et al.*, 2021a] H. Ayoobi, M. Cao, R. Verbrugge, and B. Verheij. Argue to learn: Accelerated argumentation-based learning. In *20th IEEE International Conference on Machine Learning and Applications (ICMLA)*, 2021.

[Ayoobi *et al.*, 2021b] Hamed Ayoobi, Ming Cao, Rineke Verbrugge, and Bart Verheij. Argumentation-based online incremental learning. *IEEE Transactions on Automation Science and Engineering*, pages 1–15, 2021.

[Bach *et al.*, 2015] Sebastian Bach, Alexander Binder, Grégoire Montavon, Frederick Klauschen, Klaus-Robert Müller, and Wojciech Samek. On pixel-wise explanations for non-linear classifier decisions by lrp. *PLOS ONE*, 10(7):1–46, 07 2015.

[Baroni *et al.*, 2015] Pietro Baroni, Marco Romano, Francesca Toni, Marco Aurisicchio, and Giorgio Bertanza. Automatic evaluation of design alternatives with quantitative argumentation. *Argument & Computation*, 6(1):24–49, 2015.

[Baroni *et al.*, 2018] Pietro Baroni, Antonio Rago, and Francesca Toni. How many properties do we need for gradual argumentation? In *Proceedings of the Thirty-Second Conference on Artificial Intelligence (AAAI)*, 2018.

[Blackard and Dean, 1999] Jock A. Blackard and Denis J. Dean. Comparative accuracies of artificial neural networks and discriminant analysis in predicting forest cover types from cartographic variables. *Computers and Electronics in Agriculture*, 24(3):131–151, 1999.

[Cayrol and Lagasque-Schiex, 2005] Claudette Cayrol and Marie-Christine Lagasque-Schiex. Graduality in argumentation. *J. Artif. Intell. Res.*, 23:245–297, 2005.

[Cyras *et al.*, 2019] K. Cyras, D. Letsios, R. Misener, and F. Toni. Argumentation for explainable scheduling. In *Proceedings of the Thirty-Third AAAI Conference on Artificial Intelligence*, 2019.

[Cyras *et al.*, 2021] Kristijonas Cyras, Antonio Rago, Emanuele Albini, Pietro Baroni, and Francesca Toni. Argumentative XAI: A survey. In *Proceedings of the Thirtieth International Joint Conference on Artificial Intelligence, IJCAI 2021*, 2021.

[Darwiche and Hirth, 2020] Adnan Darwiche and Auguste Hirth. On the reasons behind decisions. In *24th European Conference on Artificial Intelligence (ECAI)*, 2020.

[Ferreira *et al.*, 2022] João Ferreira, Manuel de Sousa Ribeiro, Ricardo Gonçalves, and João Leite. Looking inside the black-box: Logic-based explanations for neural networks. In *Proceedings of the 19th International Conference on Principles of Knowledge Representation and Reasoning, KR 2022*, 2022.

[Giordano and Dupré, 2021] Laura Giordano and Daniele Theseider Dupré. Weighted defeasible knowledge bases and a multipreference semantics for a deep neural network model. In *European Conference on Logics in Artificial Intelligence (JELIA)*, 2021.

[Gonzalez, 1982] Teofilo F Gonzalez. On the computational complexity of clustering and related problems. In *System modeling and optimization*, pages 174–182. Springer, 1982.

[Guidotti *et al.*, 2019] Riccardo Guidotti, Anna Monreale, Fosca Giannotti, Dino Pedreschi, Salvatore Ruggieri, and Franco Turini. Factual and counterfactual explanations for black box decision making. *IEEE Intell. Syst.*, 34(6):14–23, 2019.

[Heo *et al.*, 2019] Juyeon Heo, Sunghwan Joo, and Taesup Moon. Fooling neural network interpretations via adversarial model manipulation. *Advances in Neural Information Processing Systems*, 32:2925–2936, 2019.

[Ignatiev *et al.*, 2019] Alexey Ignatiev, Nina Narodytska, and João Marques-Silva. Abduction-based explanations for machine learning models. In *The Thirty-Third AAAI Conference on Artificial Intelligence, AAAI*, 2019.

[Jeff Larson and Angwin, 2016] Lauren Kirchner Jeff Larson, Surya Mattu and Julia Angwin. Compas recidivism risk score data and analysis, May 2016. Republica.com.

[Liu and Lorini, 2021] Xinghan Liu and Emiliano Lorini. A logic for binary classifiers and their explanation. In *Logic*

[Louizos *et al.*, 2017] Christos Louizos, Karen Ullrich, and Max Welling. Bayesian compression for deep learning. In *Int. Conference on Neural Information Processing Systems (NIPS)*, page 3290–3300, Red Hook, NY, USA, 2017. Curran Associates Inc.

[Louizos *et al.*, 2018] Christos Louizos, Max Welling, and Diederik P. Kingma. Learning sparse neural networks through 1.0 regularization. In *Int. Conference on Learning Representations, ICLR*, 2018.

[Lundberg and Lee, 2017] Scott M Lundberg and Su-In Lee. A unified approach to interpreting model predictions. In *Int. conference on neural information processing systems*, pages 4768–4777, 2017.

[MacQueen, 1967] J MacQueen. Classification and analysis of multivariate observations. In *5th Berkeley Symp. Math. Statist. Probability*, pages 281–297, 1967.

[Marques-Silva and Ignatiev, 2022] João Marques-Silva and Alexey Ignatiev. Delivering trustworthy AI through formal XAI. In *Proceedings of the Thirty-Sixth AAAI Conference on Artificial Intelligence, AAAI*, 2022.

[Mossakowski and Neuhaus, 2018] Till Mossakowski and Fabian Neuhaus. Modular semantics and characteristics for bipolar weighted argumentation graphs. *arXiv preprint arXiv:1807.06685*, 2018.

[Potyka, 2018] Nico Potyka. Continuous dynamical systems for weighted bipolar argumentation. In *International Conference on Principles of Knowledge Representation and Reasoning (KR)*, pages 148–157, 2018.

[Potyka, 2019] Nico Potyka. Extending modular semantics for bipolar weighted argumentation. In *Int. Conference on Autonomous Agents and MultiAgent Systems (AAMAS)*, pages 1722–1730, 2019.

[Potyka, 2021] Nico Potyka. Interpreting neural networks as quantitative argumentation frameworks. In *Proceedings of the Thirty-Third AAAI Conference on Artificial Intelligence, (AAAI-21)*, 2021.

[Prabhakar and Rahimi Afzal, 2019] Pavithra Prabhakar and Zahra Rahimi Afzal. Abstraction based output range analysis for neural networks. *Advances in Neural Information Processing Systems (NeurIPS)*, 32, 2019.

[Rago *et al.*, 2016] Antonio Rago, Francesca Toni, Marco Aurisicchio, and Pietro Baroni. Discontinuity-free decision support with quantitative argumentation debates. In *International Conference on Principles of Knowledge Representation and Reasoning (KR)*, pages 63–73, 2016.

[Rao *et al.*, 2022] Sukrut Rao, Moritz Böhle, and Bernt Schiele. Towards better understanding attribution methods. In *IEEE/CVF Conference on Computer Vision and Pattern Recognition (CVPR)*, pages 10223–10232, 2022.

[Ribeiro *et al.*, 2016] Marco Tulio Ribeiro, Sameer Singh, and Carlos Guestrin. ” why should i trust you?” explaining the predictions of any classifier. In *Proceedings of the 22nd ACM SIGKDD international conference on knowledge discovery and data mining*, pages 1135–1144, 2016.

[Sanchez-Lengeling *et al.*, 2020] Benjamin Sanchez-Lengeling, Jennifer Wei, Brian Lee, Emily Reif, Peter Wang, Wesley Qian, Kevin McCloskey, Lucy Colwell, and Alexander Wiltschko. Evaluating attribution for graph neural networks. *Advances in neural information processing systems (NeurIPS)*, 33:5898–5910, 2020.

[Shih *et al.*, 2018] Andy Shih, Arthur Choi, and Adnan Darwiche. A symbolic approach to explaining bayesian network classifiers. In Jérôme Lang, editor, *Proceedings of the Twenty-Seventh International Joint Conference on Artificial Intelligence, IJCAI 2018*, 2018.

[Sukpanichnant *et al.*, 2021] Purin Sukpanichnant, Antonio Rago, Piyawat Lertvittayakumjorn, and Francesca Toni. Neural qbafs: Explaining neural networks under lrp-based argumentation frameworks. In *AIxIA 2021 - Advances in Artificial Intelligence - 20th International Conference of the Italian Association for Artificial Intelligence, Virtual Event, December 1-3, 2021, Revised Selected Papers*, volume 13196 of *Lecture Notes in Computer Science*, pages 429–444. Springer, 2021.

[Tai *et al.*, 2016] Cheng Tai, Tong Xiao, Xiaogang Wang, and E. Weinan. Convolutional neural networks with low-rank regularization. In *Int. Conference on Learning Representations (ICLR)*, page Virtual, 2016.

[Wu *et al.*, 2021] Mike Wu, Sonali Parbhoo, Michael C Hughes, Volker Roth, and Finale Doshi-Velez. Optimizing for interpretability in deep neural networks with tree regularization. *JAIR*, 72:1–37, 2021.

[Yu *et al.*, 2022] Shixing Yu, Zhewei Yao, Amir Gholami, Zhen Dong, Sehoon Kim, Michael W. Mahoney, and Kurt Keutzer. Hessian-aware pruning and optimal neural implant. In *Proceedings of the IEEE/CVF Winter Conference on Applications of Computer Vision (WACV)*, pages 3880–3891, January 2022.

[Zintgraf *et al.*, 2017] Luisa M. Zintgraf, Taco S. Cohen, Tameem Adel, and Max Welling. Visualizing deep neural network decisions: Prediction difference analysis. In *Int. Conference on Learning Representations ICLR*, page Virtual. OpenReview.net, 2017.

Supplementary Materials:

SpArX: Sparse Argumentative Explanations for Neural Networks

Hamed Ayoobi¹, Nico Potyka¹, Francesca Toni¹

¹Department of Computing, Imperial College London, United Kingdom
 {h.ayoobi, n.potyka, f.toni}@imperial.ac.uk

1 Foundations

Proof of Proposition 1

Proposition 1. *Let \mathcal{M} be an MLP with activation function φ that is invertible or ReLU. Then, for every input x , the QAF $Q_{\mathcal{M},x}$ satisfies $\mathcal{O}_x^{\mathcal{M}}(v_{l,i}) = \sigma(A_{l,i})$, where $\sigma(A_{l,i})$ denotes the final strength of $A_{l,i}$ in $Q_{\mathcal{M},x}$.*

Proof. $Q_{\mathcal{M},x}$ is acyclic by construction. For acyclic QAFs, the iterative two-step update procedure is equivalent to a simple forward pass, where each argument is updated once according to any topological ordering of the arguments [Potyka, 2019]. Given that $Q_{\mathcal{M},x}$ has the graphical structure of \mathcal{M} , a natural topological ordering is given by $A_{l,i} < A_{l',i'}$ if $l \leq l'$ and $i < i'$. The update order then corresponds to the standard forward propagation procedure in MLPs. Then, the claim follows by induction over the depth d of \mathcal{M} . For the input arguments at depth $d = 0$, we do not have any attackers or supporters. Therefore, the aggregation function will just return 0 and we have $\sigma(A_{0,i}) = \varphi(\varphi^{-1}(x_i)) = x_i = \mathcal{O}_x^{\mathcal{M}}(v_{0,i})$, which proves the base case. For the induction step, consider an argument at depth $d + 1$. We have $\sigma(A_{d+1,i}) = \varphi(\varphi^{-1}(\varphi(b_i^{d+1})) + \sum_{(A_{d,i'}, A_{d+1,i}) \in E} W_{i',i}^d \cdot \sigma(A_{d,i'})) = \varphi(b_i^{d+1} + \sum_{(A_{d,i'}, A_{d+1,i}) \in E} W_{i',i}^d \cdot \mathcal{O}_x^{\mathcal{M}}(v_{d,i'})) = \mathcal{O}_x^{\mathcal{M}}(v_{d+1,i})$, which completes the proof. \square

Motivation of Aggregation Functions

Our global aggregation function is motivated as follows. Every neuron in the original MLP \mathcal{M} is represented by a cluster in the corresponding clustered MLP μ . Ideally, we want that the output of the cluster in μ is equal to the output of all neurons in \mathcal{M} . However, obviously, this is only possible if all neurons in the cluster would have the same output in the first place. The next best thing to do is then to minimize the expected deviation. However, due to the layerwise dependencies (the activation of a neuron depends on all weights and biases in all previous layers) and non-linear activation functions, the resulting objective function does not possess a simple closed-form solution and the solution is not necessarily unique. We, therefore, choose a heuristic approach to define the aggregation functions that should result in a small, but not necessarily minimal deviation.

Instead of trying to minimize the deviation in the activations of cluster neurons and neurons in the cluster directly, we minimize the deviation of the parameters (weights and biases) that cause the deviation in the activations. For the particular case that all neurons in a cluster have equal parameters (and therefore equal outputs), this minimization would result in the common parameters and the deviation would be 0. Based on these considerations, we now derive the global bias and weight aggregation functions.

For biases, given a cluster neuron v_C with corresponding bias b , we want to minimize

$$\sum_{v_{l,i} \in C} (b - b_i^l)^2. \quad (1)$$

As usual, we use the fact that the partial derivatives at a minimum must be 0. By setting the derivative with respect to b to 0 and solving for b , we find that we must have

$$b = \frac{\sum_{v_{l,i} \in C} b_i^l}{|C|}, \quad (2)$$

which corresponds to our bias aggregation function.

Thinking about the weights is slightly more complicated because the weights represent the connection strength between two cluster neurons. When considering an edge (v_{C_1}, v_{C_2}) in the clustered MLP, we have to take account of the fact that every neuron $v_2 \in C_2$ is potentially influenced by all neurons in the previous layer. In particular, it is potentially influenced by all $v_1 \in C_1$. Hence, while v_2 will potentially receive $|C_1|$ inputs from the neurons in C_1 , v_{C_2} will receive only one input from v_{C_1} . When comparing the weight w of the edge (v_{C_1}, v_{C_2}) with a weight $W_{j,i}^l$ between neurons $v_{l,i} \in C_1$ and $v_{l,j} \in C_2$, it is therefore important to divide w by $|C_1|$ (since (v_{C_1}, v_{C_2}) represents $|C_1|$ edges, it should be $|C_1|$ times larger than the weight of the individual edges). Hence, given a pair of clusters (C_1, C_2) with corresponding weight w , we want to minimize

$$\sum_{v_{l,i} \in C_1} \sum_{v_{l+1,j} \in C_2} (W_{j,i}^l - \frac{w}{|C_1|})^2. \quad (3)$$

Setting the derivative with respect to w to 0 yields the necessary condition

$$0 = -2 \cdot \sum_{v_{l,i} \in C_1} \sum_{v_{l+1,j} \in C_2} (W_{j,i}^l - \frac{w}{|C_1|}). \quad (4)$$

Dividing both sides of the equation by 2 and rearranging terms yields

$$\sum_{v_{l,i} \in C_1} \sum_{v_{l+1,j} \in C_2} W_{j,i}^l = \sum_{v_{l,i} \in C_1} \sum_{v_{l+1,j} \in C_2} \frac{w}{|C_1|} = |C_2| \cdot w. \quad (5)$$

Dividing by $|C_2|$ leads to the expression in our weight aggregation function

$$w = \frac{1}{|C_2|} \sum_{v_{l,i} \in C_1} \sum_{v_{l+1,j} \in C_2} W_{j,i}^l. \quad (6)$$

2 Experiments

This section includes more detailed experimental results for Section 7. The code to run the experiments is part of this submission and will be made publicly available upon acceptance.

Performance of Trained Models

Tables 1, 2, 3, and 4 show the average F1-scores of the trained MLPs using 90% of the data for training the models. Only for the `forest covtype` dataset, increasing the number of hidden layers and the number of hidden neurons in an MLP leads to a higher F1-score.

#Layers	#Neurons		
	100	200	500
1	0.9667	0.9667	0.9667
2	0.9667	0.9667	0.9667
3	0.9667	0.9667	0.9667
4	0.9667	0.9667	0.9667
5	0.9667	0.9667	0.9667

Table 1: Average F1-scores for trained MLPs with different numbers of hidden layers (#Layers) and hidden neurons (#Neurons) using the `iris` dataset.

#Layers	#Neurons		
	100	200	500
1	0.9349	0.9177	0.9183
2	0.9445	0.9349	0.8914
3	0.9082	0.9260	0.8758
4	0.8834	0.8820	0.9539
5	0.8741	0.9013	0.9355

Table 2: Average F1-scores for trained MLPs with different numbers of hidden layers (#Layers) and hidden neurons (#Neurons) using the `cancer` dataset.

#Layers	#Neurons		
	100	200	500
1	0.7009	0.7064	0.6996
2	0.6934	0.6660	0.6622
3	0.6699	0.6738	0.6690
4	0.6715	0.6561	0.6701
5	0.6623	0.6873	0.6714

Table 3: Average F1-scores for trained MLPs with different numbers of hidden layers (#Layers) and hidden neurons (#Neurons) using the `COMPAS` dataset.

#Layers	#Neurons		
	100	200	500
1	0.8035	0.8324	0.8795
2	0.8622	0.9068	0.9457
3	0.8862	0.9272	0.9519
4	0.9025	0.9356	0.9507
5	0.9100	0.9400	0.9529

Table 4: Average F1-scores for trained MLPs with different numbers of hidden layers (#Layers) and hidden neurons (#Neurons) using the `forest covtype` dataset.

Scalability with Other Compression Ratios

Tables 5, 6, and 7 show the unfaithfulness comparison of the local explanations of SpArX with LIME using 20%, 40%, and 60% compression ratios for the `forest covtype` dataset, respectively.

#Layers	Method	#Neurons		
		100	200	500
1	LIME	0.2375	0.2919	0.3123
	SpArX	0.0000	0.0004	0.0000
2	LIME	0.2509	0.2961	0.3638
	SpArX	0.0018	0.0008	0.0031
3	LIME	0.3130	0.3285	0.3127
	SpArX	0.0017	0.0016	0.0000
4	LIME	0.3395	0.3459	0.3243
	SpArX	0.0001	0.0044	0.0000
5	LIME	0.3665	0.3178	0.3288
	SpArX	0.0004	0.0048	0.0000

Table 5: Evaluating scalability of SpArX: local input-output unfaithfulness of SpArX (with 20% compression ratio) and LIME using various MLP architectures with different numbers of hidden layers (#Layers) and neurons (#Neurons) using the `forest covtype` dataset.

#Layers	Method	#Neurons		
		100	200	500
1	LIME	0.2375	0.2919	0.3123
1	SpArX	0.0000	0.0006	0.0000
2	LIME	0.2509	0.2961	0.3638
2	SpArX	0.0012	0.0026	0.0031
3	LIME	0.3130	0.3285	0.3127
3	SpArX	0.0028	0.0021	0.0000
4	LIME	0.3395	0.3459	0.3243
4	SpArX	0.0001	0.0044	0.0000
5	LIME	0.3665	0.3178	0.3288
5	SpArX	0.0030	0.0045	0.0000

Table 6: Evaluating scalability of SpArX: local input-output unfaithfulness of SpArX (with 40% compression ratio) and LIME using various MLP architectures with different numbers of hidden layers (#Layers) and neurons (#Neurons) using the `forest covtype` dataset.

Run-time

Table 8 shows the average run-time in seconds of SpArX (using different compression ratios) and LIME for generating local explanations. These results show that on average generating a deep local explanation with SpArX takes longer than generating a shallow (input-output) explanation with LIME. In this experiment, we have used an Intel(R) Core(TM) i7-7700HQ CPU @ 2.80GHz with 16GB of RAM using a windows 10 (education) operating system. SpArX explanations do not use GPU or CPU multiprocessing.

#Layers	Method	#Neurons		
		100	200	500
1	LIME	0.2375	0.2919	0.3123
1	SpArX	0.0000	0.0005	0.0000
2	LIME	0.2509	0.2961	0.3638
2	SpArX	0.0017	0.0015	0.0034
3	LIME	0.3130	0.3285	0.3127
3	SpArX	0.0038	0.0026	0.0000
4	LIME	0.3395	0.3459	0.3243
4	SpArX	0.0026	0.0048	0.0000
5	LIME	0.3665	0.3178	0.3288
5	SpArX	0.0028	0.0059	0.0002

Table 7: Evaluating scalability of SpArX: local input-output unfaithfulness of SpArX (with 60% compression ratio) and LIME using various MLP architectures with different numbers of hidden layers (#Layers) and neurons (#Neurons) using the `forest covtype` dataset.

#Layers	Method	#Neurons		
		100	200	500
1	LIME	0.1612	0.1633	0.1645
1	SpArX	0.0747	0.1047	0.3999
2	LIME	0.1612	0.1633	0.1645
2	SpArX	0.1865	0.2269	0.8985
3	LIME	0.1612	0.1633	0.1645
3	SpArX	0.2881	0.3809	1.5887
4	LIME	0.1612	0.1633	0.1645
4	SpArX	0.3430	0.4368	2.5342
5	LIME	0.1612	0.1633	0.1645
5	SpArX	0.3729	0.5275	3.3333

Table 8: Average run-times in seconds (over different compression ratios 20%, 40%, 60%, 80%) of SpArX and LIME (in seconds) for generating local explanations from MLPs with different numbers of hidden layers (#Layers) and neurons (#Neurons) for the `forest covtype` dataset.

An Example of Local Explanation with SpArX

Using the same MLP used in Figure 2 for the COMPAS dataset as in the paper, the *local explanations* of an example, with 20% and 85% compression ratios, are shown in Figure 1. Figure 1b is more interpretable than Figure 1a since it has fewer cluster-neurons. The label for this example is 0 which means that the criminal has not recommitted the crime in a two-year period. The local explanation shows this fact by emphasising C_2 as a stronger attacker than the supporter C_3 . C_2 says that since the sex of the criminal is female, she has only 1 prior, she has no recidivism, she has custody time of 1 to 9 days and the crime was theft, she will not recommit the crime in a two years period. Again, this example shows that SpArX can produce explanations for MLPs well beyond the shallow input-output explanations that are standard in the state-of-the-art.

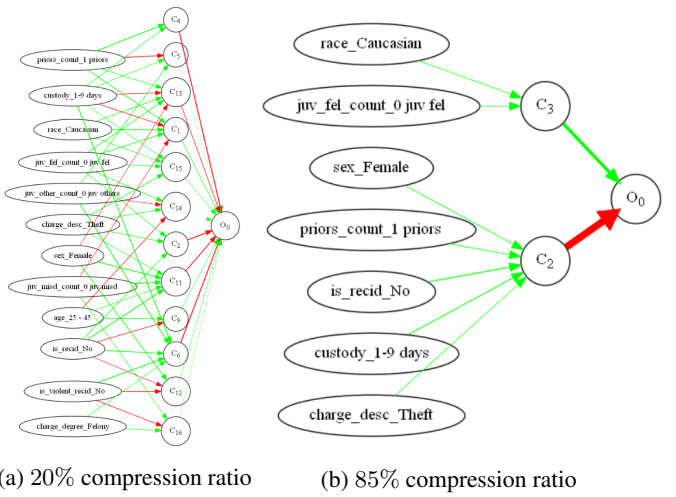


Figure 1: Local explanations by SpArX of an MLP with 20% and 85% compression ratios for the COMPAS dataset.

References

[Potyka, 2019] Nico Potyka. Extending Modular Semantics for Bipolar Weighted Argumentation. In *International Conference on Autonomous Agents and MultiAgent Systems (AAMAS)*, pages 1722–1730, 2019.